

# Differential Deposition of Fluorescently Tagged Cholesterol on Commercial Contact Lenses Using a Novel In Vitro Eye Model

Hendrik Walther<sup>1</sup>, Chau-Minh Phan<sup>1</sup>, Lakshman N. Subbaraman<sup>1</sup>, and Lyndon Jones<sup>1</sup>

<sup>1</sup> Centre for Ocular Research & Education (CORE) – formerly Centre for Contact Lens Research (CCLR), School of Optometry and Vision Science, Waterloo, Ontario, Canada

**Correspondence:** Hendrik Walther, Centre for Ocular Research & Education (CORE), School of Optometry and Vision Science, 200 University Ave West, Waterloo, ON, N2L 3G1, Canada. email: hendrik.walther@uwaterloo.ca

**Received:** 10 November 2017

**Accepted:** 17 February 2018

**Published:** 5 April 2018

**Keywords:** cholesterol; lipid; contact lens; daily disposable; eye model; deposition; laser scanning confocal microscopy; conventional hydrogel; silicone hydrogel

**Citation:** Walther H, Phan C-M, Subbaraman LN, Jones L. Differential deposition of fluorescently tagged cholesterol on commercial contact lenses using a novel in vitro eye model. *Trans Vis Sci Tech.* 2018;7(2):18, <https://doi.org/10.1167/tvst.7.2.18>

Copyright 2018 The Authors

**Purpose:** We evaluate the differences in lipid uptake and penetration in daily disposable (DD) contact lenses (CL) using a conventional “in-vial” method compared to a novel in vitro eye model.

**Methods:** The penetration of fluorescently labelled 22-(N-(7-Nitrobenz-2-Oxa-1,3-Diazol-4-yl)Amino)-23,24-Bisnor-5-Cholen-3beta-OI (NBD)-cholesterol on three silicone hydrogel (SH) and four conventional hydrogel (CH) DD CLs were investigated. CLs were incubated for 4 and 12 hours in a vial, containing 3.5 mL artificial tear solution (ATS), or were mounted on an in vitro eye-blink platform designed to simulate physiologic tear flow (2 mL/24 hours), tear volume and “simulated” blinking. Subsequently, CLs were analyzed using laser scanning confocal microscopy and ImageJ.

**Results:** Penetration depth and fluorescence intensities of NBD-cholesterol varied between the incubation methods as well as lens materials. Using the traditional vial incubation method, NBD-cholesterol uptake occurred equally on both sides of all lens materials. However, using our eye-blink model, cholesterol penetration was observed primarily on the anterior surface of the CLs. In general, SH lenses showed higher intensities of NBD-cholesterol than CH materials.

**Conclusions:** The traditional “in-vial” incubation method exposes the CLs to an excessively high amount of ATS, which results in an overestimation for cholesterol deposition. Our model, which incorporates important ocular factors, such as intermittent air exposure, small tear volume, and physiological tear flow between blinks, provides a more natural environment for in vitro lens incubation.

**Translational Relevance:** In vitro measurements of CLs are a common approach to predict their interactions and performance on the eye. Traditional methods, however, are rudimentary. Therefore, this study presents a novel in vitro model to evaluate CLs, which consequently will enhance elucidations of the interactions between CLs and the eye.

## Introduction

Contact lens (CL) dropout remains a pressing concern for the CL industry, with discomfort being a primary factor.<sup>1–3</sup> Consequently, there is an increasing demand on manufacturers to continually produce safer and more comfortable CLs.<sup>4–6</sup> The first generation of soft CLs, consisting of poly(2-hydroxyethyl methacrylate; pHEMA) and its derivatives, were

relatively comfortable, but unfortunately did not permit adequate oxygen transmission for the cornea to function optimally.<sup>7,8</sup> This problem was addressed in the late 1990s with the introduction of silicone hydrogel (SH) CL<sup>9–11</sup> materials that provided relatively high oxygen transmissibility.<sup>9–11</sup> However, due to the hydrophobic siloxane moieties within SH CLs, these materials suffered from reduced surface wettability,<sup>12–14</sup> and increased lipid deposition.<sup>15–20</sup> As a

**Table 1.** Properties of CH Used in the Study

	1-DAY ACUVUE MOIST	BioMedics 1 Day	Biotrue 1 Day	DAILIES AquaComfort Plus
United States adopted name (USAN)	etafilcon A	ocufilcon B	nesofilcon A	nelfilcon A
Manufacturer	Johnson & Johnson	CooperVision	Bausch+Lomb	Alcon
Water content (%)	58%	52%	78%	69%
FDA group	IV	IV	II	II
Center thickness (mm)	0.08	0.07	0.05	0.10
Oxygen transmissibility ( $\times 10^{-9}$ )	25.5	24	24	26
Principal monomers	HEMA, MA	HEMA, PVP, MA	HEMA, NVP	FMA, PVA, PEG

FMA, N-formylmethyl acrylamide; HEMA, hydroxyethyl methacrylate; MA, methacrylic acid; PEG, polyethylene glycol; PVA, polyvinyl alcohol; PVP, polyvinyl pyrrolidone; NVP, N-vinylpyrrolidone.

result, these lenses were not as comfortable as initially expected.

Despite extensive research over the past five decades, the paradigm for CL discomfort remains unclear, likely due to the multifactorial nature of comfort.<sup>21</sup> One potential hypothesis suggests that discomfort manifests from the deposition of tear components, such as lipids, on the lens over time, which leads to changes within and on the surface of the lens.<sup>17,22,23</sup> One strategy to overcome the complications associated with long-term lipid deposition is to switch to daily disposable (DD) lens wear. Even then, lipid deposition from short-term or daily wear modality still could lead to end-of-day discomfort.<sup>24</sup>

To investigate this phenomenon, studies historically have systematically investigated factors that can influence lipid deposition on CLs.<sup>20,22,24,25</sup> Important elements to consider are tear film (TF) lipid concentration, exposure time, properties of the lens material, and interactions between various TF components with the lens.<sup>18,20,22,26–28</sup> Previously, we also have shown that intermittent air exposure from a simulated blinking motion also is a crucial factor in influencing the degree of lipid deposition.<sup>29</sup>

The challenge in elucidating the mechanisms of TF deposition in vivo is to adequately model a similar scenario in vitro. In the past, for CL deposition studies, researchers used simplistic models by immersing lenses in a vial containing 3.5 mL simulated tear fluid containing the component of interest.<sup>20,22,24</sup> However, on the ocular surface, the tear volume is estimated to be only  $7 \pm 2 \mu\text{L}$ ,<sup>30</sup> with a tear exchange rate of 0.95 to 1.55  $\mu\text{L}/\text{min}$ .<sup>31</sup> Thus, it is apparent that the previous models are too rudimentary, lacking not only the tear flow component, but the incubation volume also far exceeds physiologic levels. Thus, to

further our understanding of TF deposition, a better in vitro model is necessary.

Studies evaluating lipid deposition on CLs traditionally have focused on quantifying the amount of lipids deposited on the lens.<sup>17–20,25,29</sup> To gain further insights on tear deposition, it also is of interest to evaluate the patterns of lipid deposition and penetration through the lens over time. The use of laser scanning confocal microscopy (LSCM) has been used previously to map protein penetration on the surface and matrix of CLs using fluorescently labeled proteins.<sup>32,33</sup> The ability to visualize lipid penetration in different CL materials may help explain the variations in comfort experienced between different CLs. We characterized the penetration of fluorescently-tagged cholesterol on commercially available DD CLs using a novel ocular model,<sup>34</sup> which simulates tear volume, tear flow, and blinking, and compared the results to the standard vial incubation method.

## Materials and Methods

### CLs and Pretreatment

Four commercially available conventional hydrogel (CH) DD CLs (etafilcon A [Johnson & Johnson, Brunswick, NJ], ocufilcon B [CooperVision, Pleasanton, CA], nesofilcon A [Bausch+Lomb, Bridgewater, NJ], nelfilcon A [Alcon, Ft. Worth, TX]) and three SH lenses (delefilcon A [Alcon], somofilcon A [CooperVision], and narafilcon A [Johnson & Johnson]) were evaluated in the study. All lenses had a dioptric power of  $-3.00$  and base curve of 8.5 or 8.6 mm, obtained from the manufacturer in the original packaging. Tables 1 and 2 detail the properties of the

**Table 2.** Properties of SH Used in the Study

	DAILIES TOTAL1®	clariti™ 1day	1-DAY ACUVUE® TruEye®
United States adopted name (USAN)	delefilcon A	somofilcon A	narafilcon A
Manufacturer	Alcon	CooperVision	Johnson & Johnson
Water content (%)	33% (surface >80%)	56%	46%
FDA group	V	V	V
Center thickness (mm)	0.09	0.07	0.09
Oxygen transmissibility ( $\times 10^{-9}$ )	156.0	86	118.0
Principal monomers	Not disclosed	Not disclosed	MPDMS, DMA, HEMA, siloxane macromer, TEGDMA, PVP

DMA, N,N-dimethylacrylamide; MPDMS, monofunctional polydimethylsiloxane; TEGDMA, tetraethyleneglycol dimethacrylate.

CH and SH CLs, respectively. Before all incubation studies, all CLs were removed from their packaging solutions and soaked in 5 mL phosphate-buffered saline (PBS) for 24 hours while shaking at 30 revolutions per minute (rpm) to remove excess packaging solution. After the 24-hour soaking, the CLs were removed from the pretreatment solution and were blotted on lens paper to remove any excess liquid.

### Artificial Tear Solution

To deposit the investigational lenses with TF lipids and to determine subsequent lipid penetration patterns, our laboratory exposed the study lenses, regardless of which incubation method was applied, to an artificial tear solution (ATS) containing relevant lipids. The composition of the ATS has been reported previously by our group.<sup>25</sup> Briefly, it contains various mucins, urea, salts, glucose, proteins (lysozyme and albumin), and various lipids (oleic acid methyl ester, cholesterol, triolein, phosphatidylcholine, cholesteryl oleate, and oleic acid).<sup>25</sup>

### Fluorescently Tagged Cholesterol

Cholesterol and its derivatives are one of the primary lipid deposits found on CLs, and, thus, it was chosen as the representative lipid for this study.<sup>19,28,35–37</sup> Fluorescently-tagged 22-(N-(7-Nitrobenz-2-oxa-1,3-diazol-4-yl)amino)-23,24-bisnor-5-cholen-3 $\beta$ -ol-cholesterol (NBD-cholesterol; Fig. 1), obtained from Avanti Polar Lipids, Inc. (Alabaster, AL), was used to visualize the deposition and penetration of cholesterol into CLs. For this study, NBD-cholesterol was dissolved at a physiologic

concentration of 1.9 mg/mL in a cholesterol-free solution of ATS.

### Ocular Flow Model

Our in vitro model (OcuFlow) consists of a two-piece model that includes a “corneal/scleral” piece and an “eyelid” component, spaced 250  $\mu$ m apart. The templates for the eye models were designed using a computer-aided drawing software (Solid Works 2013), and printed using 3-dimensional (3-D) printing technology.<sup>34</sup> The resulting 3-D printed molds (PC-ABS; polycarbonate-acrylonitrile-butadiene-styrene) were filled with polydimethylsiloxane (PDMS) and cured at 75°C for 1 hour. The corneal and the eyelid pieces then were mounted on a special clip, which attaches to our blink platform.

The platform consists of two mechanical actuators. The first motor moves the eyelid laterally to simulate closing of the eye, spread of the TF, and intermittent air exposure (Fig. 2A). The second motor rotates the corneal piece circularly when the two eye pieces come together to simulate the rubbing action produced during blinking (Fig. 2B). Additionally, the system is connected to a microfluidic syringe pump (PHD; Harvard Apparatus, Holliston, MA), which is at-

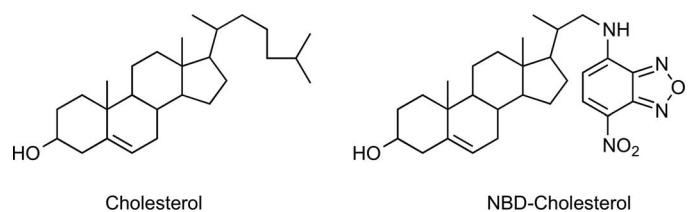


**Figure 1.** Chemical structure of cholesterol (386.65 g/mol) and NBD-cholesterol (494.63 g/mol).<sup>38</sup>

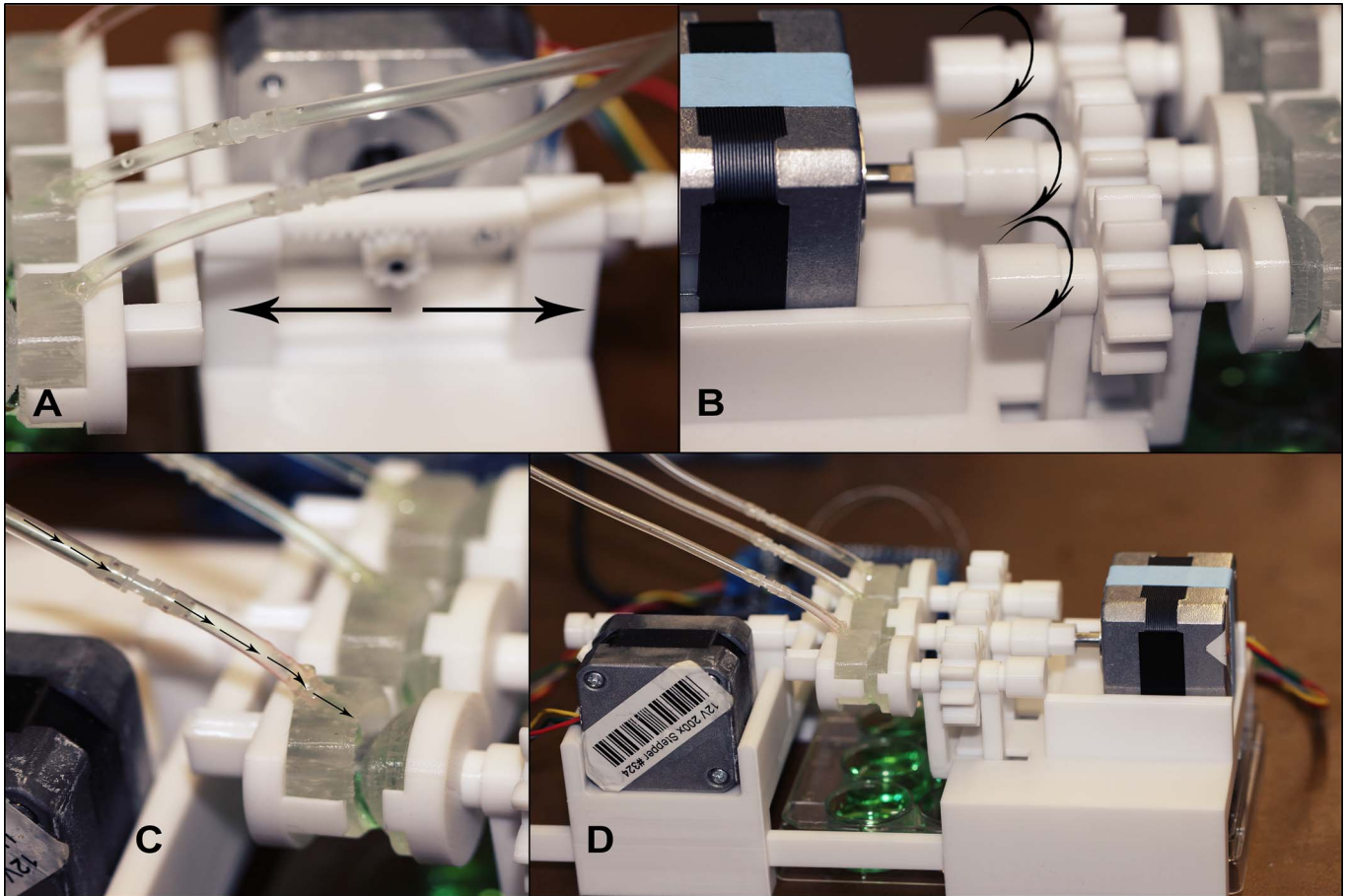


**Figure 2.** Lateral motion produces intermittent air exposure (A). Circular motion simulates rubbing action during blinking (B). TF infusion into eyelid (C). OcuFlow platform (D).

tached directly to the artificial eyelids of the platform (Fig. 2C) and injects ATS into the eye models at a physiologic flow rate of  $1.3 \mu\text{L}/\text{min}$ . The general setup of the model with attachment to the microfluidic system is shown in Figure 2D.<sup>34</sup>

### Experimental Outline

For the vial incubation condition (1), six lenses of each type were immersed in a vial containing 3.5 mL ATS with NBD-cholesterol for 12 hours at room temperature with shaking. For the eye model condition (2), six lenses of each type were placed on the OcuFlow model and allowed to run for 12 hours at room temperature with a flow rate at  $1.3 \mu\text{L}/\text{min}$  ( $2 \text{ mL}/24 \text{ hours}$ ).

At 4 and 12 hours, three lenses of each type were removed from each experimental condition, blot dried on lens paper, and prepared for imaging. These time intervals were chosen to correspond to typical short wearing times found in part-time wearers of DD

lenses and an all-day daily CL wear time period. Using a hole-punch, 5 mm diameter discs were punched out from the center of the CLs. The lens discs then were mounted carefully onto a piece of  $22 \times 40 \times 1 \text{ mm}$  Fisherbrand microscope glass cover slip (Fisher Scientific, Pittsburgh, PA). Then,  $40 \mu\text{L}$  PBS was carefully pipetted onto the lens disc, and a second glass cover slip was placed carefully on top. To secure the cover slip onto the microscope slide, a small amount of clear nail polish was applied to the sides of the cover glass using a pipette tip.

### Confocal Microscopy

To image the slides, a Zeiss LSM 510 Meta LSCM (Zeiss, Inc., Toronto, Canada) was used to excite the NBD-cholesterol with an argon laser at 488 nm and to capture the emitted fluorescence at its peak wavelength of 528 nm using a band pass filter of 505 to 530 nm. The LSCM captured a series of consecutive images spaced  $0.5 \mu\text{m}$  apart. The resulting

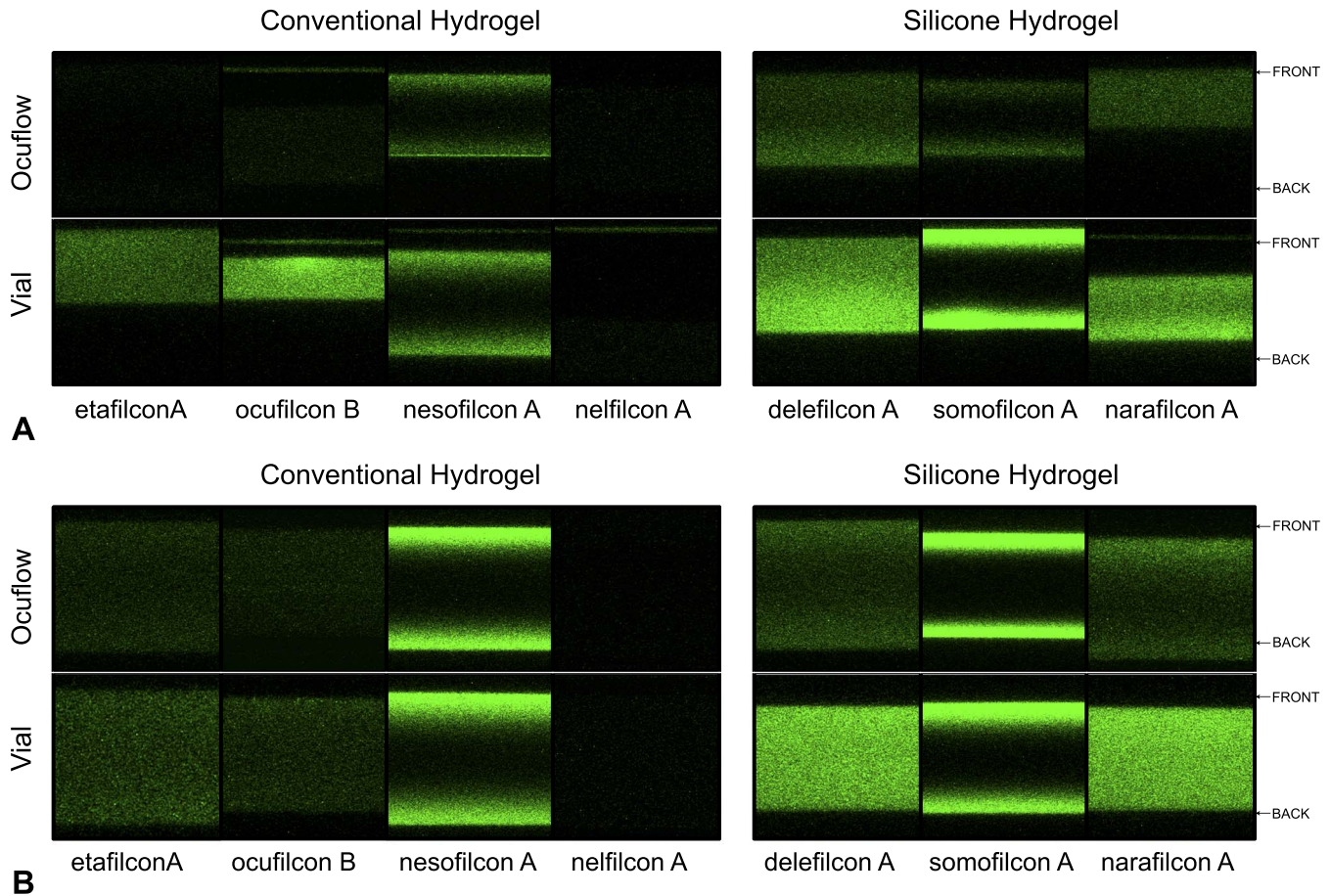


**Figure 3.** Confocal images showing a cross-section of etafilcon A, nelfilcon A, nesofilcon A, ocufilcon, delefilcon A, somofilcon A, narafilcon A after incubation with NBD-cholesterol in the vial and OcuFlow model after 4 (A) and 12 (B) hours.

images were rendered into a two-dimensional cross-section using the ZEN 2009 light software (Zeiss). The fluorescence was recorded for every fourth image per sample using ImageJ (National Institutes of Health [NIH], Bethesda, MD) and the subsequent data were averaged and corrected for the autofluorescence from the control lenses soaked in PBS and plotted on a histogram. Based on this plot, the depth of cholesterol penetration into the CL material over time was determined. By sustaining the identical laser settings for all CLs, a direct relationship can be drawn between an increase of relative intensity of fluorescence (RIF) values and NBD-cholesterol sorption on the CLs.

### Statistical Analysis

IBM SPSS Statistics 23 for Macintosh (IBM Corp., Armonk, NY) software was used to conduct repeated measures analysis of variance (RM-ANOVA) and post

hoc Tukey's multiple comparisons to test the impact of the incubation methods, CL materials, and incubation times on the lipid penetration. Statistical differences were considered significant for a  $P$  value of  $<0.05$ . The graphs were plotted using GraphPad Prism version 6.0h for Macintosh (GraphPad Software, La Jolla, CA).

## Results

The RIF of accumulated NBD-cholesterol varied greatly between the tested lens materials and tested incubation methods. A collage of the penetration patterns and a graphic illustration of the results are shown in Figures 3 and 4, respectively. The results of the performed RM-ANOVA are shown in Table 3 and revealed that all three test variables were statistically significant; individually (within) and between their interactions ( $P \leq 0.045$ ).

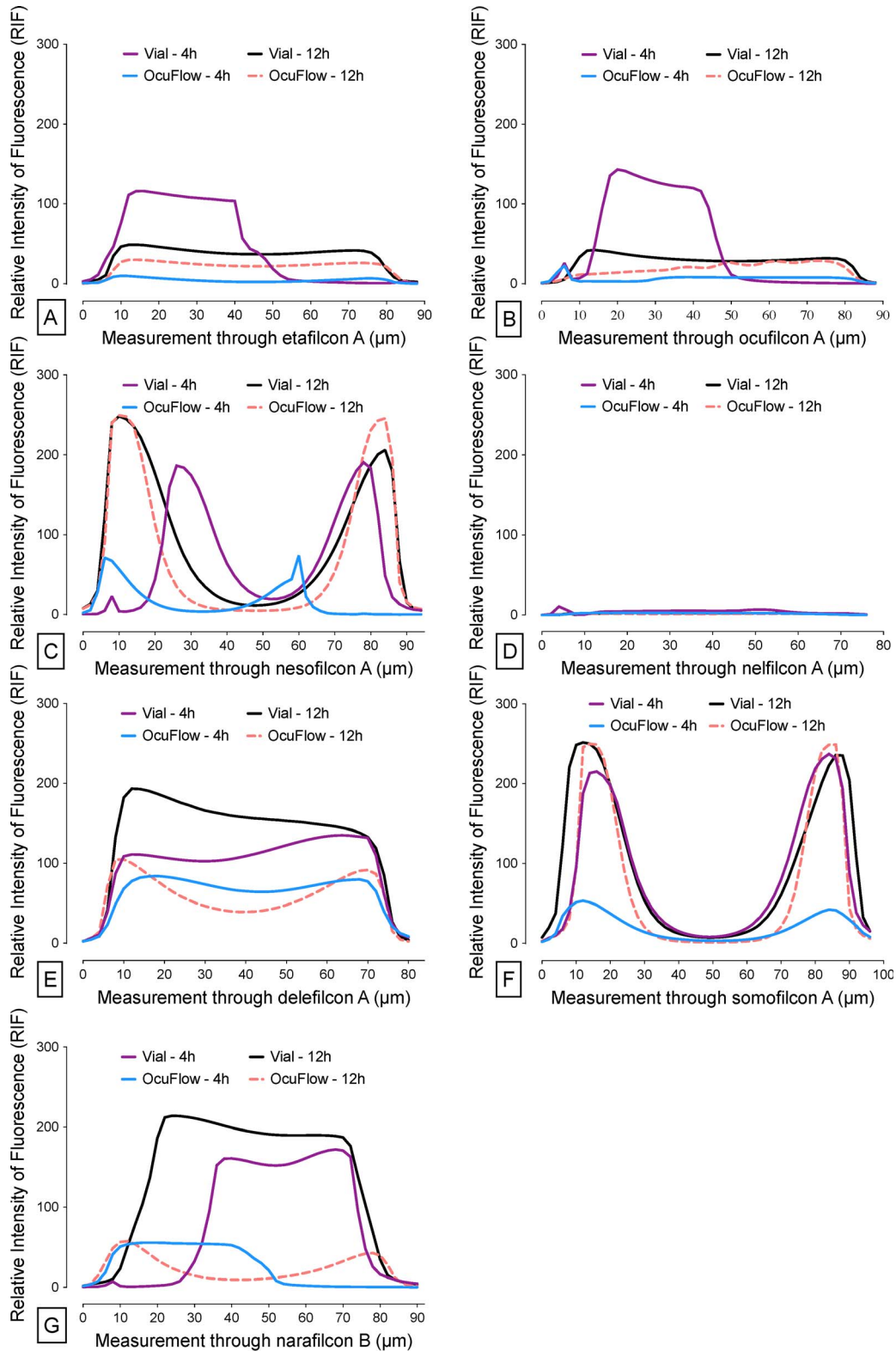


**Figure 4.** Histograms representing the different incubation methods: OcuFlow after 4 (blue line) and 12 (broken red line) hours, vial incubation after 4 (purple line) and 12 (black line) hours; as well as depth of absorption of NBD-cholesterol of various contact lenses: etafilcon A (A), nelfilcon A (B), nesofilcon A (C), ocuflcon A (D), delefilcon A (E), somofilcon A (F), naraflcon A (G). The values plotted are the relative intensity fluorescence values (RIF).

**Table 3.** Repeated Measures ANOVA Statistical Results for Cholesterol Penetration Comparing Various Incubation Methods and CL Materials

Variable	Sum of Squares	Degrees of Freedom	Mean Square	F	P
Incubation methods	1,094,750.82	1	1,094,750.82	615.43	<0.001
CL materials	2,287,925.12	6	381,320.85	90.33	<0.001
Incubation times	200,928.78	1	200,928.78	47.60	<0.001
Incubation methods × CL materials	475,027.12	6	79,171.19	44.507	<0.001
CL materials × incubation times	193,438.91	6	32,239.82	7.64	<0.001
Incubation methods × incubation times	7,148.49	1	7,148.49	4.02	0.045
Incubation methods × CL materials × incubation times	295,658.03	6	49,276.34	27.701	<0.001
Error (incubation methods)	2,844,359.78	1599	1,778.84		

### Impact of CL Material

Overall, SH lens materials accumulated significantly more ( $P \leq 0.001$ ) of the fluorescently-labeled lipid than CHs, with the exception of nesofilcon A CLs ( $P \geq 0.209$ ), which showed similar amounts of accumulated NBD-cholesterol as the somofilcon A and narafilcon A lens materials. The general pattern found, after pooling all data points for each CL material and statistically comparing between them, was: delefilcon A > somofilcon A  $\geq$  nesofilcon A  $\geq$  narafilcon A > etafilcon A > ocufilecon B > nelfilecon A, with no statistically significant differences between the SH lenses ( $P \geq 0.117$ ). Within the CH materials, however, the differences in accumulated cholesterol were statistically significant ( $P \leq 0.003$ ), except between etafilcon A and ocufilecon B ( $P = 0.992$ ).

After 4 hours of vial incubation, the deposition sequence was the same as the previously listed general pattern. However, these differences were not statistically significant between all SH lenses ( $P \geq 0.582$ ), the SH lenses and nesofilcon A ( $P \geq 0.721$ ), as well as between etafilcon A and narafilcon A ( $P = 0.130$ ), nesofilcon A ( $P = 0.141$ ), and ocufilecon B ( $P = 1.000$ ). The pattern after the 12-hour vial incubation varied slightly and was: delefilcon A > narafilcon A > somofilcon A > nesofilcon A > etafilcon A > ocufilecon B > nelfilecon A. All of those differences were statistically significant ( $P \leq 0.012$ ), except between delefilcon A and narafilcon A ( $P = 1.000$ ), somofilcon A and nesofilcon A ( $P = 0.989$ ), and ocufilecon B and nelfilecon A ( $P = 0.092$ ).

For the OcuFlow incubation method and after 4

hours, the pattern was: delefilcon A > narafilcon A > somofilcon A > nesofilcon A > ocufilecon B > etafilcon A > nelfilecon A. All of the differences were significant ( $P \leq 0.001$ ), except between somofilcon A and narafilcon A ( $P = 0.342$ ) and etafilcon A ( $P = 1.000$ ), narafilcon A and nesofilcon A ( $P = 0.451$ ), etafilcon A and ocufilecon B ( $P = 1.000$ ) and nelfilecon A ( $P = 0.978$ ), and between ocufilecon B and nelfilecon A ( $P = 0.855$ ). After 12 hours of incubation, the pattern varied: nesofilcon A > somofilcon A > delefilcon A > etafilcon A > narafilcon A > ocufilecon B > nelfilecon A. All differences were statistically significant, except between nesofilcon A, somofilcon A ( $P = 0.973$ ), and delefilcon A ( $P = 0.475$ ); between delefilcon A, somofilcon A ( $P = 0.827$ ), and etafilcon A ( $P = 0.064$ ); between narafilcon A and etafilcon A ( $P = 1.000$ ); and between ocufilecon B, narafilcon A ( $P = 1.000$ ), etafilcon A ( $P = 0.957$ ), and nelfilecon A ( $P = 0.328$ ).

Interestingly, the NBD-labeled cholesterol permeated through the entire thickness of the SH lens materials; the sole exception was in somofilcon A lenses, where the lipid only accumulated on the anterior and posterior margins (Figs. 3A, 3B). Unexpectedly, the CH lens material nesofilcon A revealed the same pattern of cholesterol penetration using both in vitro methods. Also, etafilcon A and ocufilecon A showed noteworthy penetration patterns after 4 hours of incubation with the vial method, where the NBD-cholesterol was found to deposit in the front section of those lens materials. These penetration patterns, however, subsided after 12 hours and lipid penetrated through the entire lens

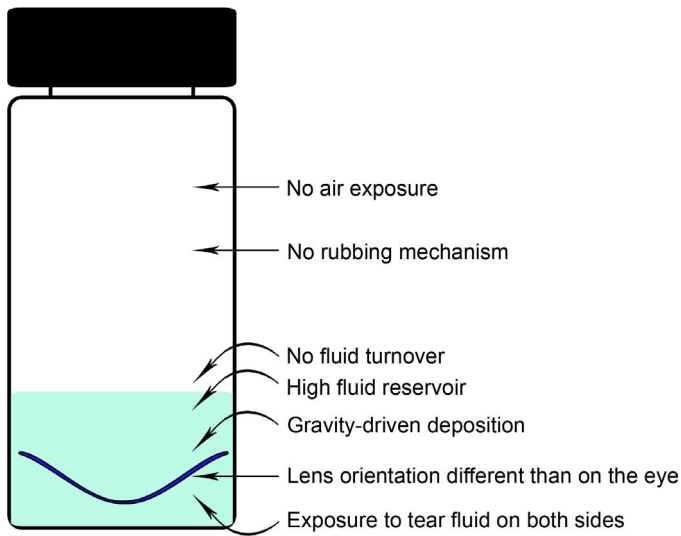


**Figure 5.** Drawbacks of using a simple vial model to evaluate CLs.

material thickness (Fig. 3B) for both incubation methods.

### Impact of Incubation Method

Based on the RIF and subsequent to both incubation times (4 and 12 hours), the uptake of the lipid was elevated considerably after 12 hours compared to the 4-hour exposure time for most lens materials. Figures 3 and 4 depict substantial differences in NBD-cholesterol between our OcuFlow model and the common vial incubation method, with a superior amount of uptake and penetration using the latter in vitro procedure ( $P < 0.001$ ). In particular, the general pattern of NBD-cholesterol accumulation for the incubation methods was “vial 12 hours” > “vial 4 hours” > “OcuFlow 12 hours” > “OcuFlow 4 hours.” All differences were statistically significant ( $P \leq 0.007$ ), except between the incubation times of the vial method ( $P = 0.109$ ).

Comparing the differences between the incubation methods within each CL material, the order of the general pattern changed slightly; nevertheless, the traditional vial method always showed greater amounts of accumulated NBD-cholesterol over the OcuFlow platform. Interestingly, somofilcon A, delefilcon A, nesofilcon A, and ocufilcon B showed higher rates of accumulated NBD-cholesterol after 4 hours of vial incubation compared to 12 hours. This, however, was only statistically significant for delefilcon A and ocufilcon B CLs ( $P \leq 0.001$ ). Most of the CLs accumulated the lowest amount of lipid after the 4-hour incubation using the in vitro platform, except for narafilcon A, which showed the least overall

amount of NBD-cholesterol after 12 hours of incubation with the OcuFlow, which, however, was not statistically significant ( $P = 0.833$ ) compared to the 4-hour time point.

## Discussion

In recent years, researchers have recognized the various limitations<sup>39–44</sup> of using a vial as an in vitro method for evaluating their interactions with TF components (Fig. 5). Subsequently, to better simulate the ocular environment, several unique in vitro eye models have been developed, such as inclusion of a microfluidic tear replenishment component,<sup>39–44</sup> intermittent air exposure,<sup>29</sup> and/or a mechanism of in vivo fouling of soft CLs.<sup>45</sup> Not surprisingly, the results generated from these experiments are very different than those obtained with the conventional vial model and might more closely resemble in vivo data.<sup>29,39–45</sup> Our unique eye model incorporates multiple key elements of the ocular environment, including tear flow, tear volume, air exposure, and mechanical rubbing, to provide the best simulated environment possible for in vitro CL evaluation.<sup>34</sup>

Being able to correctly visualize the localization of lipid deposits on CLs provides a better understanding on how the deposition of certain tear elements could progressively lead to discomfort. Previous research has been limited to quantifying lipid deposits on CLs, which provided useful data for comparing the relative performance of different CLs.<sup>17–20,24,25,29</sup> However, to fully understand the mechanism leading to discomfort, it also is important to characterize how lipids penetrate the lens material over time.

Conventional methods of evaluating TF deposition on CLs have been performed in vials. As shown in Figure 5, there are several drawbacks when CLs are evaluated in this manner, which may significantly skew the results of lipid deposition on CLs. In particular, the high incubation volume and incorrect horizontal orientation of the CL will facilitate lipid deposition on the CL, leading to an overestimation of lipid deposits. Not surprisingly, penetration and fluorescence intensity of NBD-cholesterol for all materials were considerably higher in the vial than the eye model, especially after 4 hours of incubation time. Furthermore, we also observed uncharacteristic deposition patterns for two CH, etafilcon A and ocufilcon B, in the vial, but not in the eye model. Typically, CH are hydrophilic and, therefore, do not absorb a high quantity of lipids.<sup>17–20,25,29</sup> However, as seen in Figure 3, more cholesterol penetration was



seen in etafilcon A and ocufilecon B within their lens matrix when incubated using a vial at 4 hours. After 12 hours of incubation time, the uncharacteristic deposition pattern for these two CHs subsided and the fluorescence intensity of NBD-cholesterol decreased. We speculated that this effect could be due to the diffusion of the lipid through the lens materials over time. Most likely, there was no further accumulation of cholesterol within the 4- and 12-hour time points, but instead more of a “spreading” (i.e., balancing out) of the lipid within the CL materials. Therefore, the total amount of lipid deposited may be similar between the time-points; however, the fluorescence intensity appears vastly different because the NBD-cholesterol is distributed more uniformly after 12 than 4 hours. This inconsistency also highlights the drawback of using a vial in which the CL is positioned horizontally. In this orientation, the deposition of TF on the CL is facilitated partially by gravity, rather than the material properties of the CL. In contrast, these artifacts were not observed in the OcuFlow, which can be attributed to the unique vertical orientation of the CL on the model.

For most parts, there still was a strong agreement between the vial and the OcuFlow model in regards to the overall pattern of lipid penetration and deposition on the materials. For instance, both conditions showed that there was no lipid penetration in the matrix of the lens for nesofilcon A (CH) and somofilcon A (SH) at either the 4- or 12-hour time point. With the exception of nelfilcon A, cholesterol deposition and penetration increased between 4 and 12 hours for all lens types in the vial and OcuFlow model. Similar and consistent patterns in lipid penetration also were observed for nelfilcon A, delefilcon A, and narafilcon A. The penetration and fluorescence intensity were higher in SH than CH CLs in both models. Therefore, results from the vial experiments could still be considered relevant for evaluating the relative performance of CLs in regards to lipid deposition.<sup>24</sup>

Upon closer examination of Figure 3, it appears that the investigational lenses are of different thicknesses, especially nesofilcon A. It could be possible that CLs might dehydrate more while using the OcuFlow platform compared to the vial method, which could explain the differences in thickness. However, although we did not measure the amount of dehydration after lens incubation, we believe that the amount of dehydration occurring is minimal, as the CLs are constantly exposed to fluid during lens incubation. On-eye data by Efron and Brennan et

al.<sup>46–48</sup> showed that CLs dehydrate minimally while being worn, which we believe is similar to what is experienced when they are placed in the OcuFlow model. In general, lens thickness varies between lens materials and manufacturers, due to their differing designs and water content. The lens thicknesses, however, were consistent within each CL material (as seen in Fig. 4), which provides further evidence that the CLs do not undergo significant dehydration.

For commercially available CH and SH lenses, the effective pore sizes are approximately 150 nm.<sup>49</sup> The molecular size of cholesterol is estimated to be 1.6 nm across its length.<sup>50</sup> Since none of the DD CLs used in this study were surface coated, we expected that NBD-cholesterol would be able to penetrate throughout the lens material.<sup>50</sup> Interestingly, for some lens materials, such as nesofilcon A (CH) and somofilcon A (SH), cholesterol was localized mostly on the surface of the lens, but not within the polymer matrix, even after 12 hours. The reasons for this lipid localization is unclear. We propose that it could be due to a structural arrangement of the polymers within these lenses, which favors binding to NBD-cholesterol at the surface. Furthermore, this interaction is likely not solely due to hydrophobic interactions, but rather the result of side chains between the polymer and lipid. Other lenses, such as delefilcon A and narafilcon A, also exhibited a similar deposition pattern after 12 hours for the OcuFlow system. Interestingly, nelfilcon A showed almost no sign of cholesterol penetration even after 12 hours.

An important property that cannot be simulated in a vial incubation is the formation of the pre- and post-lens TF, created when the CL sits on the cornea in vivo. While the pre-lens TF is replenished continually, there is very little tear exchange occurring behind the post-lens TF.<sup>51–53</sup> Consequently, we initially expected that there would be minimal lipid deposition occurring on the posterior side of the lens. To date, few studies have investigated the differential deposition of TF on CLs, but this observation has been noted previously with the deposition of vitronectin.<sup>54</sup> However, even using the OcuFlow model, we were unable to observe a significant difference between the front and back surface depositions for NBD-cholesterol. This suggests that there is enough CL distortion and movement to allow for sufficient tear fluid to deposit on the back surface of the lens.<sup>55</sup> One of the problems with our current model is that the eyepiece is synthesized from PDMS, a highly hydrophobic material. As such, the post-lens seal created between the eyepiece and CL in our model may be less tight

and, thus, may not yet achieve the perfect fit that an in vivo CL does on the eye. As a result, as the eyelid piece presses on the corneal piece, there is enough pressure to force fluid beneath the lens. We predict that using a more hydrophilic material for the eyepiece will generate a different penetration profile for the back surface of the CL and this warrants further experimentation.

LSCM can provide useful insights on how tear components are absorbed within a lens material.<sup>32,33</sup> However, one main drawback in using fluorescently-labeled probes, such as NBD-cholesterol, is the assumption that the labeled compound will behave similarly as its native counterpart. In the case of NBD-cholesterol, the fluorophore contains functional groups not found on the native lipid, which may interact differently with the lens materials. In addition, the fluorescently tagged lipid (494.63 g/mol) is significantly higher than the mass of cholesterol (386.65 g/mol). To our knowledge, there are no studies that compare the sorption of cholesterol and NBD-cholesterol on CLs. However, a study evaluating sorption of fluorescently-labeled proteins on hydrogels has shown that CLs adsorb labeled proteins much higher than native proteins, and the effect is significantly pronounced for silicone hydrogels.<sup>56</sup> Consequently, quantitative determinations of lipid depositions based on fluorescently-tagged lipids may be unreliable. However, for visualizing deposition patterns on CLs, we do not expect major significant differences between NBD-cholesterol and cholesterol, as both molecules are relatively small and hydrophobic.

In conclusion, the OcuFlow system presented in this study can be used as a model to evaluate lipid deposition on CLs. The platform mimics key ocular parameters and can replace conventional vial-based studies to provide better insights on the performance of CLs on the eye. The localization of lipid deposits and penetration on a CL, in tandem with the amount deposited, may have a significant role in determining CL discomfort. The current system described here also can be extended to evaluate deposition of other tear components.

## Acknowledgments

Supported by Canadian Optometric Education Trust Fund (COETF) and the NSERC 20/20 Network for the Development of Advanced Ophthalmic Materials.

Disclosure: **H. Walther**, None; **C.-M. Phan**, None; **L.N. Subbaraman**, None, **L. Jones**, None

## References

1. Young G, Veys J, Pritchard N, Coleman S. A multi-centre study of lapsed contact lens wearers. *Ophthalmic Physiol Opt.* 2002;22:516–527.
2. Dumbleton K, Woods CA, Jones LW, Fonn D. The impact of contemporary contact lenses on contact lens discontinuation. *Eye Contact Lens.* 2013;39:93–99.
3. Pritchard N, Fonn D, Brazeau D. Discontinuation of contact lens wear: a survey. *Int Contact Lens Clin.* 1999;26:157–162.
4. Nicolson PC, Vogt J. Soft contact lens polymers: an evolution. *Biomaterials.* 2001;22:3273–3283.
5. Tighe B. Silicone hydrogels: structure, properties and behaviour. In: Sweeney D, ed. *Silicone Hydrogels: Continuous Wear Contact Lens.* 2. Oxford: Butterworth-Heinemann; 2004:1–27.
6. Tighe B. Contact lens materials. In: Phillips A, Speedwell L, eds. *Contact Lenses*, 5th ed. Edinburgh: Butterworth-Heinemann; 2006:59–78.
7. Holden BA. The Glenn A. Fry Award lecture 1988: the ocular response to contact lens wear. *Optom Vis Sci.* 1989;66:717–733.
8. Brennan NA, Coles ML. Extended wear in perspective. *Optom Vis Sci.* 1997;74:609–623.
9. Dumbleton KA, Chalmers RL, Richter DB, Fonn D. Vascular response to extended wear of hydrogel lenses with high and low oxygen permeability. *Optom Vis Sci.* 2001;78:147–151.
10. Covey M, Sweeney DF, Terry R, Sankaridurg PR, Holden BA. Hypoxic effects on the anterior eye of high-Dk soft contact lens wearers are negligible. *Optom Vis Sci.* 2001;78:95–99.
11. Stapleton F, Stretton S, Papas E, Skotnitsky C, Sweeney DF. Silicone hydrogel contact lenses and the ocular surface. *Ocul Surf.* 2006;4:24–43.
12. Jones L, Subbaraman L, Rogers R, Dumbleton K. Surface treatment, wetting and modulus of silicone hydrogels. *Optician.* 2006;232:28–34.
13. Read ML, Morgan PB, Kelly JM, Maldonado-Codina C. Dynamic contact angle analysis of silicone hydrogel contact lenses. *J Biomat Appl.* 2011;26:85–99.
14. Maldonado-Codina C, Morgan PB. In vitro water wettability of silicone hydrogel contact lenses determined using the sessile drop and

- captive bubble techniques. *J Biomed Mat Res A*. 2007;83:496–502.
15. Jones L, Senchyna M, Glasier MA, Schickler J, Forbes I, Louie D, et al. Lysozyme and lipid deposition on silicone hydrogel contact lens materials. *Eye Contact Lens*. 2003;29(suppl): S75–S79; discussion S83–S84, S192–S194.
  16. Ghormley N, Jones L. Managing lipid deposition on silicone hydrogel lenses. *Contact Lens Spectrum*. 2006;21:21.
  17. Lorentz H, Jones L. Lipid deposition on hydrogel contact lenses: how history can help us today. *Optom Vis Sci*. 2007;84:286–295.
  18. Carney FP, Nash WL, Sentell KB. The adsorption of major tear film lipids in vitro to various silicone hydrogels over time. *Invest Ophthalmol Vis Sci*. 2008;49:120–124.
  19. Pucker AD, Thangavelu M, Nichols JJ. In vitro lipid deposition on hydrogel and silicone hydrogel contact lenses. *Invest Ophthalmol Vis Sci*. 2010; 51:6334–6340.
  20. Lorentz H, Heynen M, Trieu D, Hagedorn SJ, Jones L. The impact of tear film components on in vitro lipid uptake. *Optom Vis Sci*. 2012;89:856–867.
  21. Nichols KK, Redfern RL, Jacob JT, et al. The TFOS International Workshop on Contact Lens Discomfort: report of the definition and classification subcommittee. *Invest Ophthalmol Vis Sci*. 2013;54:TFOS14–TFOS19.
  22. Walther H, Lorentz H, Heynen M, Kay L, Jones LW. Factors that influence in vitro cholesterol deposition on contact lenses. *Optom Vis Sci*. 2013;90:1057–1065.
  23. Nichols JJ. Deposition on silicone hydrogel lenses. *Eye Contact Lens*. 2013;39:20–23.
  24. Walther H, Subbaraman L, Jones LW. In vitro cholesterol deposition on daily disposable contact lens materials. *Optom Vis Sci*. 2016;93:36–41.
  25. Lorentz H, Heynen M, Kay LM, et al. Contact lens physical properties and lipid deposition in a novel characterized artificial tear solution. *Mol Vis*. 2011;17:3392–3405.
  26. Bontempo AR, Rapp J. Protein-lipid interaction on the surface of a hydrophilic contact lens in vitro. *Curr Eye Res*. 1997;16:776–781.
  27. Iwata M, Ohno S, Kawai T, Ichijima H, Cavanagh HD. In vitro evaluation of lipids adsorbed on silicone hydrogel contact lenses using a new gas chromatography/mass spectrometry analytical method. *Eye Contact Lens*. 2008; 34:272–280.
  28. Zhao Z, Carnt NA, Aliwarga Y, et al. Care regimen and lens material influence on silicone hydrogel contact lens deposition. *Optom Vis Sci*. 2009;86:251–259.
  29. Lorentz H, Heynen M, Khan W, Trieu D, Jones L. The impact of intermittent air exposure on lipid deposition. *Optom Vis Sci*. 2012;89:1574–1581.
  30. Mishima S, Gasset A, Klyce SD Jr, Baum JL. Determination of tear volume and tear flow. *Invest Ophthalmol*. 1966;5:264–276.
  31. Furukawa RE, Polse KA. Changes in tear flow accompanying aging. *Am J Optom Physiol Opt*. 1978;55:69–74.
  32. Luensmann D, Glasier MA, Zhang F, Bantsev V, Simpson T, Jones L. Confocal microscopy and albumin penetration into contact lenses. *Optom Vis Sci*. 2007;84:839–847.
  33. Luensmann D, Zhang F, Subbaraman L, Sheardown H, Jones L. Localization of lysozyme sorption to conventional and silicone hydrogel contact lenses using confocal microscopy. *Curr Eye Res*. 2009;34:683–697.
  34. Phan CM, Walther H, Gao H, Rossy J, Subbaraman LN, Jones L. Development of an in vitro ocular platform to test contact lenses. *J Vis Exp*. 2016:e53907.
  35. Maziarz EP, Stachowski MJ, Liu XM, et al. Lipid deposition on silicone hydrogel lenses, part I: quantification of oleic acid, oleic acid methyl ester, and cholesterol. *Eye Contact Lens*. 2006;32: 300–307.
  36. Saville JT, Zhao Z, Willcox MD, Blanksby SJ, Mitchell TW. Detection and quantification of tear phospholipids and cholesterol in contact lens deposits: the effect of contact lens material and lens care solution. *Invest Ophthalmol Vis Sci*. 2010;51:2843–2851.
  37. Heynen M, Lorentz H, Srinivasan S, Jones L. Quantification of non-polar lipid deposits on senofilcon a contact lenses. *Optom Vis Sci*. 2011; 88:1172–1179.
  38. Sparrow CP, Patel S, Baffic J, et al. A fluorescent cholesterol analog traces cholesterol absorption in hamsters and is esterified in vivo and in vitro. *J Lipid Res*. 1999;40:1747–1757.
  39. Tieppo A, Pate KM, Byrne ME. In vitro controlled release of an anti-inflammatory from daily disposable therapeutic contact lenses under physiological ocular tear flow. *Eur J Pharm Biopharm*. 2012;81:170–177.
  40. Ali M, Horikawa S, Venkatesh S, Saha J, Hong JW, Byrne ME. Zero-order therapeutic release from imprinted hydrogel contact lenses within in vitro physiological ocular tear flow. *J Control Release*. 2007;124:154–162.

41. White CJ, McBride MK, Pate KM, Tieppo A, Byrne ME. Extended release of high molecular weight hydroxypropyl methylcellulose from molecularly imprinted, extended wear silicone hydrogel contact lenses. *Biomaterials*. 2011;32:5698–5705.
42. Kaczmarek JC, Tieppo A, White CJ, Byrne ME. Adjusting biomaterial composition to achieve controlled multiple-day release of dexamethasone from an extended-wear silicone hydrogel contact lens. *J Biomat Sci Polym Ed*. 2014;25:88–100.
43. Liao Y-T, Yao H, Lingley A, Parviz B, Otis BP. A 3 $\mu$ W CMOS glucose sensor for wireless contact-lens tear glucose monitoring. *Ieee J Solid-St Circ*. 2012;47:335–344.
44. Mohammadi S, Postnikoff C, Wright AM, Gorbet M. Design and development of an in vitro tear replenishment system. *Ann Biomed Eng*. 2014;42:1923–1931.
45. Peng CC, Fajardo NP, Razunguzwa T, Radke CJ. In vitro spoilation of silicone-hydrogel soft contact lenses in a model-blink cell. *Optom Vis Sci*. 2015;92:768–780.
46. Efron N, Young G. Dehydration of hydrogen contact lenses in vitro and in vivo. *Ophthalmic Physiol Opt*. 1988;8:253–256.
47. Efron N, Brennan NA, Bruce AS, Duldig DI, Russo NJ. Dehydration of hydrogel lenses under normal wearing conditions. *CLAO J*. 1987;13:152–156.
48. Brennan NA, Efron N, Bruce AS, Duldig DI, Russo NJ. Dehydration of hydrogel lenses: environmental influences during normal wear. *Am J Optom Physiol Opt*. 1988;65:277–281.
49. Green JA, Phillips KS, Hitchins VM, et al. Material properties that predict preservative uptake for silicone hydrogel contact lenses. *Eye Contact Lens*. 2012;38:350–357.
50. Hofsass C, Lindahl E, Edholm O. Molecular dynamics simulations of phospholipid bilayers with cholesterol. *Biophysical J*. 2003;84:2192–2206.
51. Paugh JR, Stapleton F, Keay L, Ho A. Tear exchange under hydrogel contact lenses: methodological considerations. *Invest Ophthalmol Vis Sci*. 2001;42:2813–2820.
52. Lin MC, Soliman GN, Lim VA, et al. Scalloped channels enhance tear mixing under hydrogel contact lenses. *Optom Vis Sci*. 2006;83:874–878.
53. Muntz A, Subbaraman LN, Sorbara L, Jones L. Tear exchange and contact lenses: a review. *J Optom*. 2015;8:2–11.
54. Tighe BJ, Franklin V, Graham C, Mann A, Guillon M. Vitronectin adsorption in contact lens surfaces during wear. Locus and significance. *Adv Exp Med Biol*. 1998;438:769–773.
55. Maki KL, Ross DS. Exchange of tears under a contact lens is driven by distortions of the contact lens. *Integr Comp Biol*. 2014;54:1043–1050.
56. Guan A, Li Z, Phillips KS. The effect of fluorescent labels on protein sorption in polymer hydrogels. *J Fluoresc*. 2014;24:1639–1650.